Cluster design of M-ary orthogonal DS/CDMA cellular system with Rayleigh fading and lognormal shadowing

P.I. Dallas
F.-N. Pavlidou

Indexing terms: Cluster design, Rayleigh fading, Lognormal shadowing, M-ary orthogonal DS/CDMA cellular system

Abstract: Performance analysis is carried out for a cluster of a M-ary orthogonal DS/CDMA cellular system. The bit error rate (BER) is evaluated for both the forward and the reverse link, considering a wideband frequency selective channel with Rayleigh fading and lognormal shadowing. Both cases of power control (perfect and imperfect) within each cell are examined. Coherent and noncoherent RAKE receivers are studied for the forward and the reverse link, respectively, through appropriate numerical techniques calculating the target integrals. Owing to the channel model complexity, an equivalent lognormal distribution has to be introduced to make the calculations more convenient. An increased user accommodation capability, in comparison with the one cell study, results from the overall analysis of the system.

1 Introduction

Two major problems in personal communication systems (PCN) are the multiple access problem (multiple transmissions of active users on the shame transmission medium), and the bandwidth efficiency (number of users accommodated over an acceptable GOS link) [1, 2]. A promising technique for the multiple access problem is the code division multiple access (CDMA) [1] which is currently under discussion for application in third-generation mobile radio systems [3–6]. In these systems, the requirements for an enhanced bandwidth efficiency are more imperative, so M-ary orthogonal signalling techniques constitute a very attractive solution, since it can be shown that M-ary signalling improves bandwidth efficiency, and a reduction of the required signal to noise ratio per bit for a specified error probability can be achieved [7–10].

Cluster analysis has appeared recently in a number of papers. An overview of cellular DS/CDMA was presented by Lee [11]. Gilhousen *et al.* [12] have provided a capacity analysis taking into account the path loss and the lognormal shadowing but ignoring the multipath fading. On the other hand, Milstein *et al.*, in [13], assumed only the Rayleigh model and coherent BPSK modulation and carried out a mathematical analysis, evaluating the error probabilities for both communication links: base-to-mobile link and vice versa. Also, Misser and Prasad [14] have considered a microcellular mobile radio system, where they examined the multipath effects, but in a CPSK receiver with Rician shadowing. Perfect power control is assumed in almost all the references in the literature apart from [13]. The effects of imperfect power control on capacity, throughput and delay for a sectorised narrowband cellular slotted DS/CDMA system were presented by Jansen and Prasad [15]. A more general model for the evaluation for a sectorised cluster of the uplink and downlink channels considering the multipath fading, the path loss and the background noise has been developed by Stuber and Kchao [16] for a coherent receiver with binary signalling. Finally, Tonguz and Wang [17] have studied the effect of power control on the performance of cellular CDMA for both links, considering flat Rayleigh fading and UHF attenuation.

M-ary orthogonal signalling in a wideband mobile radio environment is a very recent research topic and only the reverse link of single cell structures has been examined [8, 10, 18, 19]. Also, apart from [19] only fast fading models have been considered. Therefore, due to the lack in the literature of a complete cluster analysis of M-ary orthogonal signalling, a system with perfect and imperfect power control terms of BER performance for a frequency selective channel with multipath Rayleigh fading and lognormal shadowing is investigated. The study is carried out for both the links: forward (base station to mobile) and reverse (mobile to base station) to make clear the impact of multiple cells on such a system. An M-ary coherent receiver with maximal ratio combiner (MRC) is used in the forward link, while for the reverse link a noncoherent M-ary receiver with square law detection combining is selected. Perfect power control is first applied in each cell to assure the equalisation of the received powers within each cell, but this condition is finally relaxed so that the sensitivity of the system to imperfect power control can be studied in the cluster domain.

The complexity of the mathematical model leads us to approximate the joint probability density function of Rayleigh-lognormal with an equivalent lognormal

IEE Proceedings online no. 19971243
Paper first received 8th February and in revised form 9th December 1996
The authors are with the Telecommunications Division, Department of Electrical & Computer Engineering, Faculty of Technology, Aristotle University of Thessaloniki, Greece

according to a previous publication [20]. The approximation is found to be very satisfactory, depending on the number of resolvable paths.

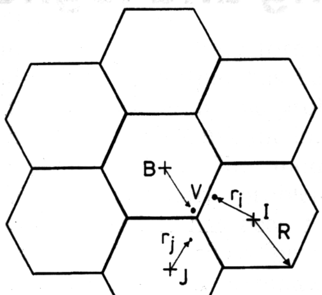

Fig. 1 *Forward link DS/CDMA system geometry, showing 'home' cell B and neighbouring cells I and J*

2 Forward link analysis

The cellular CDMA channel is modelled as a multipath Rayleigh with lognormal shadowing over L paths. A cluster of cells with radius R is studied assuming DS/CDMA coherent M-ary orthogonal signalling with K users in each cell. Each user is assigned a set $\vec{S}^k$ of M orthogonal sequences with length N and period T:

$$\vec{S}^k = \{s_1^k, s_2^k, ..., s_m^k, ..., s_M^k\} \tag{1}$$

Mobile users at the edge of a cell moving along the route $\overline{BV}$ (Fig. 1) are examined. This route has been chosen because it represents the worst case situation [21]. When the mobile is close to the vertex of the 'home' cell, the received signal consists of the $K - 1$ interfering signals from the 'home' cell, denoted as B, together with other K interfering signals from the two more closest cells denoted as I and J (Fig. 1). We assumed that the interference from other cells is negligible following the concept in [17]. Although the channel model is multipath, all signals are assumed to fade in unison within each path. Hence, the received signal at the mobile receiver can be written as

$$\begin{aligned} r(t) = \eta(t) + \sqrt{2P_S}\Bigg[\sum_{l=1}^{L}\beta_{B,l}\Bigg\{ & s_m^1(t-\tau_{B,l}) \\ & \times \exp[j\omega_c(t-\tau_{B,l}) + j(\varphi_{B,l}+\theta_{B,1})] \\ & + \sum_{k=2}^{K}(U_m^k(t-\tau_{B,l})\exp[j\omega_c(t-\tau_{B,l})+j(\varphi_{B,l}+\theta_{B,k})])\Bigg\}\Bigg] \\ & + \sum_{i=1}^{K}\sum_{l=1}^{L}\sqrt{2P_S\partial(r_i)}[\beta_{I,l}U_m^i(t-\tau_{I,l}) \\ & \times \exp[j\omega_c(t-\tau_{I,l})+j(\varphi_{I,l}+\theta_{I,i})]] \\ & + \sum_{j=1}^{K}\sum_{l=1}^{L}\sqrt{2P_S\partial(r_j)}[\beta_{J,l}U_m^j(t-\tau_{J,l}) \\ & \times \exp[j\omega_c(t-\tau_{J,l})+j(\varphi_{J,l}+\theta_{J,j})]] \end{aligned} \tag{2}$$

The first term in eqn. 2 represents the additive white Gaussian noise with two-sided spectral density $N_0/2$. The remaining terms represent the desired signal and the interference resulting either from mobiles in the 'home' cell or from mobiles in the two neighbouring cells. P_S is the transmitted power at the base station. $\partial(r_i)$ and $\partial(r_j)$ are parametric functions due to the lack of a unified power control scheme throughout the cluster and are proportional to r_i^{-n}. r_i is the distance between the ith mobile and its own base station, and n is the path loss coefficient depending on the environment structure, usually chosen to be equal to 4. $s_m^1(t - \tau_{B,l})$ is the mth symbol transmitted by the first user. $U_m^\xi(t - \tau_{\rho,l})$, ($\xi = k, i, j$ and $\rho = B, I, J$), represents the concatenation of interference during the intervals $[\tau_{\rho,l} - T, \tau_{\rho,l})$ and $[\tau_{\rho,l}, \tau_{\rho,l} + T)$ [7]. θ_k is the carrier phase introduced by the transmitter and ω_c is the common angular frequency. $\tau_{\rho,l}$, $\varphi_{\rho,l}$ is the path delay and path phase of the lth path in the ρth cell and are random variables uniformly distributed in the region [0, T) and [0, 2π). Finally, $\beta_{\rho,l}$ is the path gain of the lth path and the ρth cell and is user independent since all signals fade in unison.

We have assumed two types of fading: fast (Rayleigh) and slow (lognormal) fading [19] with characteristic parameters the mean area power $\xi = \ln \mu$ and the standard deviation σ. To facilitate the mathematical analysis, we have approximated the joint probability function of multipath Rayleigh and lognormal shadowing with an equivalent lognormal distribution that is given by

$$f_{eq}(x) = \frac{1}{\sigma_L x\sqrt{2\pi}}\exp\left(-\frac{(\ln x - \xi_L)}{2\sigma_L^2}\right) \tag{3}$$

where $\xi_L = \ln \mu_L$ and $\mu_L = \mu\sqrt{[L^3/(L+1)]}$ and $\sigma_L = \sqrt{\{\sigma^2 + \ln[(L + 1)/L]\}}$. The proof is given in the Appendix.

The optimum receiver for wideband fading multipath signals is a RAKE one which consists of M matched filters (for the M symbols, respectively) with L active taps, Fig. 2 [22]. The decision variable is based on the maximal ratio combining structure. Without loss of generality, we choose arbitrarily the first user of the 'home' cell as the desired one and the ith path as the reference path, so $\tau_{B,v} = 0$ and $\theta_{B,v} = 0$.

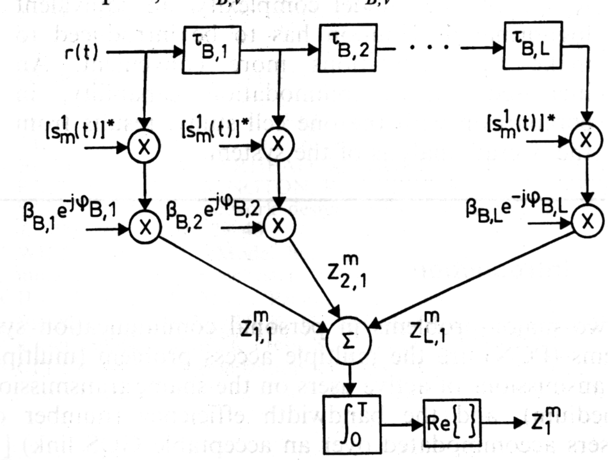

Fig. 2 *Coherent type of RAKE receiver with MRC for forward link*

The output Z_{i1}^m for the vth path and the mth symbol is given by:

$$Z_{v1}^m = \text{Re}\left\{\int_0^T r(t)\exp(-j\omega_c t)\beta_{B,v}\exp(-j\varphi_{B,v})[s_m^1(t)]^* dt\right\} \tag{4}$$

After some mathematical manipulations, the previous form can be written:

$$Z_{v1}^\lambda = \begin{cases} \sqrt{\frac{P_S}{2}}T\beta_{B,v}^2 + N_c^B + N_c^I + N_c^J + \eta_I(t) & \lambda = m \\ N_c^B + N_c^I + N_c^J + \eta_I(t) & \lambda \neq m \end{cases} \tag{5a}$$

where

$$N_c^B = \sqrt{\frac{P_S}{2}}T\sum_{k=1}^{K}\sum_{l=1,l\neq v}^{L}\beta_{B,v}\beta_{B,l}Y_{B,k,l}^\lambda \tag{5b}$$

$$N_c^I = \sqrt{\frac{P_S}{2}}T\sum_{i=1}^{K}\sum_{l=1}^{L}\sqrt{r_i^{-n}}\beta_{B,v}\beta_{I,l}Y_{I,i,l}^\lambda \tag{5c}$$

$$N_c^J = \sqrt{\frac{P_S}{2}}T\sum_{j=1}^{K}\sum_{l=1}^{L}\sqrt{r_j^{-n}\beta_{B,v}\beta_{J,l}Y^{\lambda}_{J,j,l}} \quad (5d)$$

The first term for $\lambda = m$ in eqn. 5*a* is the desired signal and the others declare the interference and the noise. For any other symbol, there is only interference and noise. The term $Y^{\lambda}_{\rho,\zeta,l}$ represents the multiple access interference due to the mth signal and is given by [23]:

$$Y^{\lambda}_{\rho,\zeta,l} = \frac{1}{T}[b_1 R^{\rho}_{\zeta}(\tau_l) + b_0 \hat{R}^{\rho}_{\zeta}(\tau_l)]\cos\Omega_{\rho,\zeta,l} \quad (6)$$

where $\Omega_{\rho,\zeta,l} = \varphi_{\rho,l} - \varphi_{B,l} + \theta_{\rho,\zeta} - \omega_C\tau_{\rho,l}$ is the total phase. The vectors (b_1, b_0) represent two contiguous spreading codes to emphasise that the partial cross-correlation functions $R^{\rho}_{\zeta}(\tau_l)$, $\hat{R}^{\rho}_{\zeta}(\tau_l)$ refer to the interference caused to the current symbol by the previous and the succeeding ones.

The noise term is as follows:

$$\eta_I(t) = \mathrm{Re}\left\{\beta_{B,v}\exp(-j\varphi_{B,v}) \times \int_0^T [\eta(t)(s^1_m(t))^* \exp(-j\omega_c t)]\,dt\right\} \quad (7)$$

The decision variable for the mth symbol is $Z_1^m = \Sigma_{v=1}^{L} Z^m_{v1}$. Such sums for all the symbols are derived and compared, and the maximum of these outputs is selected.

2.1 Performance analysis

To evaluate the proposed system via the symbol error probability, we have to calculate the signal to noise plus interference ratio which can be written:

$$Y_s = \frac{\sum_{v=1}^{L}\beta^2_{B,v}}{\frac{N_0}{E_S} + K\left[\sum_{\substack{I=1\\I\neq v}}^{L}\beta^2_{B,v} + \mathrm{var}[r_i^{-n}Y^{\lambda}_{\rho,\zeta,I}]\left(\sum_{l=1}^{L}\beta^2_{I,l} + \sum_{l=1}^{L}\beta^2_{J,l}\right)\right]} \quad (8)$$

where $E_S = P_S T$ is the energy per symbol, while the energy per bit is given by $E_b = E_S/\log_2 M$ since $\log_2 M$ bits are transmitted with each symbol. The term $Y^{\lambda}_{\rho,\zeta,l}$ has been widely studied [23–25] and is proved to be Gaussian with variance $\mathrm{var}[Y^{\lambda}_{\rho,\zeta,l}] = 1/3N$ for rectangular chip pulse, since we have used orthogonal sequences similar to [7–9]. Alternative pulse shapes and the impact on the performance are presented in [26]. The product $\sqrt{(r_i^{-n})}\,Y^{\lambda}_{\rho,\zeta,l}$ is also zero mean Gaussian, whose variance depends on the spatial distribution of the mobiles around the base station. The locations of the mobiles are assumed to be independent uniform random variables [17] with probability density function:

$$f_r(r_i) = \begin{cases} \frac{2r_i}{R^2} & 0 \le r_i \le R \\ 0 & \text{otherwise} \end{cases} \quad (9)$$

The variance of the product can be derived as:

$$\mathrm{var}[r_i^{-n}Y^{\lambda}_{\rho,\zeta,l}] = \mathrm{var}[Y^{\lambda}_{\rho,\zeta,l}]\int_0^R\left(\sqrt{r_i^{-n}}\right)^2 f_r(r_i)dr_i$$
$$= \mathrm{var}[Y^{\lambda}_{\rho,\zeta,l}]\int_0^R\left(\sqrt{r_i^{-n}}\right)^2 \frac{2r_i}{R^2}dr_i$$
$$= \frac{1}{3N}\left|\frac{2}{R^n(2-n)}\right| \quad (10)$$

Focusing our interest on interference problems other than white noise, we can assume that $E_S/N_0 >> 1$ and the previous form can be approximated by the following:

$$Y_s \simeq \left[\frac{K}{3N}\left(1 + \left|\frac{2}{R^n(2-n)}\right|\frac{\sum_{l=1}^{L}\beta^2_{I,l} + \sum_{l=1}^{L}\beta^2_{J,l}}{\sum_{v=1}^{L}\beta^2_{B,v}}\right)\right]^{-1}$$
$$= \left[\frac{K}{3N}\left(1 + \left|\frac{2}{R^n(2-n)}\right|\frac{\chi_I + \chi_J}{\chi_B}\right)\right]^{-1} \quad (11)$$

letting $\chi_B = \Sigma_{v=1}^{L}\beta^2_{B,v}$, $\chi_I = \Sigma_{l=1}^{L}\beta^2_{I,l}$, and $\chi_J = \Sigma_{l=1}^{L}\beta^2_{J,l}$.

Applying $n = 4$, the symbol error probability conditioned on χ_B, χ_I, χ_J is given by:

$$P_e(Y_s/\chi_B, \chi_I, \chi_J) = \frac{(M-1)}{2}\mathrm{erfc}\left(\sqrt{\frac{1}{2}\left[\frac{K}{3N}\left(1 + \frac{1}{R^4}\frac{\chi_I + \chi_J}{\chi_B}\right)\right]^{-1}}\right) \quad (12)$$

Defining $w = \chi_I + \chi_J$ and $u = \chi_B$, we have to find out the joint probability of the ratio $v = w/u$. It can be proved that [27, 28]:

$$f_v(v) = \int_0^{\infty} f_w(vu) f_u(u) u\, du \quad (13)$$

According to Wilkinson's method [29, 30], the probability function $f_w(w)$ of a sum of lognormal variables is a lognormal distribution with equivalent standard deviation σ_w and mean μ_w and can be given as

$$\sigma_w^2 = \ln u_2 - 2\ln u_1 \quad (14a)$$

$$\xi_w = 2\ln u_1 - \frac{1}{2}\ln u_2 \text{ or } \mu_w = \frac{u_1^2}{\sqrt{u_2}} \quad (14b)$$

where

$$\xi_w = \ln \mu_w \quad (15a)$$

$$u_1 = \exp\left(\xi_{\chi_I} + \frac{\sigma^2_{\chi_I}}{2}\right) + \exp\left(\xi_{\chi_J} + \frac{\sigma^2_{\chi_J}}{2}\right) \quad (15b)$$

$$u_2 = \exp(2\xi_{\chi_I} + 2\sigma^2_{\chi_I}) + \exp(2\xi_{\chi_J} + 2\sigma^2_{\chi_J}) + 2\exp\left(\xi_{\chi_I} + \xi_{\chi_J} + \frac{1}{2}(\sigma^2_{\chi_I} + \sigma^2_{\chi_J})\right) \quad (15c)$$

Finally, the unconditioned symbol error probability can be written combining all the above equations as:

$$P_M = \int_0^{\infty}\frac{(M-1)}{2}\mathrm{erfc}\left(\sqrt{\frac{1}{2}\left[\frac{K}{3N}\left(1 + \frac{1}{R^4}v\right)\right]^{-1}}\right) \times \left(\int_0^{\infty} f_w(uv) f_u du\right) dv \quad (16)$$

The symbol error probability P_M can be converted to an equivalent bit error probability P_b by the following transformation:

$$P_b = \frac{2^{\log_2 M - 1}}{2^{\log_2 M} - 1}P_M \quad (17)$$

3 Reverse link analysis

We consider now the mobile-to-base station link in the same cluster structure but with a DS/CDMA noncoherent M-ary orthogonal signalling. For the reverse link analysis, the assumption of unison fading is relaxed and we have path gain, path phase and path delay, different for each user. The received signal at the base station can be written as

$$
\begin{aligned}
r(t) = \eta(t) + \sqrt{2P_S}\Bigg[&\sum_{l=1}^{L} \beta_{B,l1} s_m^1(t-\tau_{B,l1}) \\
&\times \exp[j\omega_c(t-\tau_{B,l1}) + j(\varphi_{B,l1}+\theta_{B,1})] \\
&+ \sum_{k=2}^{K}\sum_{l=1}^{L} (\beta_{B,lk} U_m^k(t-\tau_{B,lk}) \\
&\times \exp[j\omega_c(t-\tau_{B,lk}) + j(\varphi_{B,lk}+\theta_{B,k})])\Bigg] \\
&+ \sum_{i=1}^{K}\sum_{l=1}^{L} \sqrt{2P_S\partial(r_i')}\,[\beta_{I,li} U_m^i(t-\tau_{I,li}) \\
&\times \exp[j\omega_c(t-\tau_{I,li}) + j(\varphi_{I,li}+\theta_{I,i})]] \\
&+ \sum_{j=1}^{K}\sum_{l=1}^{L} \sqrt{2P_S\partial(r_j')}\,[\beta_{I,lj} U_m^j(t-\tau_{I,lj}) \\
&\times \exp[j\omega_c(t-\tau_{J,lj}) + j(\varphi_{J,lj}+\theta_{J,j})]] \qquad (18)
\end{aligned}
$$

Similarly, with the forward link analysis the first term is the desired signal and the others constitute the interference either from the same cell or from the two neighbouring cells. The functions $\partial(r_i')$ and $\partial(r')$ are similar as in the forward link but now r_i' is the distance of the ith mobile of the neighbouring cell from the base station of the 'home' cell (Fig. 3). $\beta_{\rho,l\zeta}$, $\tau_{\rho,l\zeta}$, $\varphi_{\rho,l\zeta}$ ($\rho = B, I, J$) are the path gain, the path delay and the path phase of the lth path of the kth user in the ρth cell. The channel model has been approximated again with an equivalent lognormal distribution as in the forward link case.

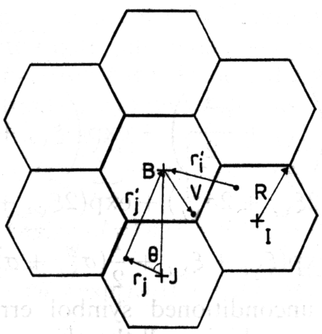

Fig. 3 *Reverse link DS/CDMA system geometry, showing 'home' cell B and neighboring cells I and J*
Mobile interferers from neighbouring cells are J and I are r'_j and r'_i, respectively

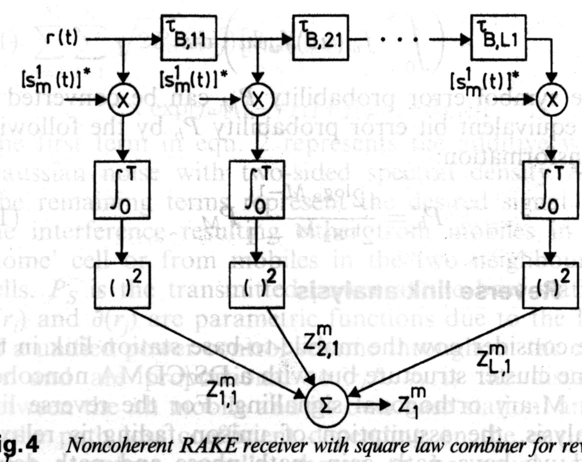

Fig. 4 *Noncoherent RAKE receiver with square law combiner for reverse link*

We will now consider the receiver for the signal transmitted by the first user. It is a RAKE demodulator with a square combining law that consists of M matched filters for the M symbols (Fig. 4) [22]. The RAKE has L active taps and the output of the mth symbol is given by:

$$Z_1^m = \sum_{v=1}^{L} |Z_{v1}^m|^2 \qquad (19)$$

where Z_{v1}^m is the matched filter output of the ith path and can be derived as follows:

$$Z_{v1}^m = \int_0^T r(t)\exp[-j\omega_c t][s_m^1(t)]^* dt \qquad (20)$$

After mathematical manipulation, the output can be written as:

$$Z_{v1}^\lambda = \begin{cases} \sqrt{\frac{P_S}{2}}T\beta_{B,v1}\cos\Omega_{B,v1} \\ \quad +N_c^B + N_c^I + N_c^J + \eta_I(t) & \lambda = m \\ N_c^B + N_c^I + N_c^J + \eta_I(t) & \lambda \neq m \end{cases} \qquad (21a)$$

where

$$N_c^B = \sqrt{\frac{P_S}{2}}T\sum_{k=1}^{K}\sum_{l=1,l\neq v}^{L} \beta_{B,lk}Y_{B,k,1}^\lambda \qquad (21b)$$

$$N_c^I = \sqrt{\frac{P_S}{2}}T\sum_{i=1}^{K}\sum_{l=1}^{L} \sqrt{r_i'}\beta_{I,li}Y_{I,i,1}^\lambda \qquad (21c)$$

$$N_c^J = \sqrt{\frac{P_S}{2}}T\sum_{j=1}^{K}\sum_{l=1}^{L} \sqrt{r_j'}\beta_{I,lj}Y_{I,j,1}^\lambda \qquad (21d)$$

The terms $Y_{\rho,\zeta,l}^\lambda$ ($\rho = B, I, J$ & $\zeta = k, i, j$) have been denoted in the forward link case. We can calculate the variance of the terms $\sqrt{(r_j'^{-n})}\ Y_{J,j1}^\lambda$ and $\sqrt{(r_i'^{-n})}\ Y_{I,i,1}^\lambda$ assuming uniform spatial traffic density [17]. Both terms have equal variances so we determine only the first. It is given that:

$$r_j' = 3R^2 + r_j^2 - 2\sqrt{3}Rr_j\cos\theta \qquad (22)$$

r_j is the distance of the adjacent interfering user to its own base station, and θ is uniformly distributed between $[0, 2\pi)$. Thus, letting $n = 4$, we have:

$$
\begin{aligned}
\mathrm{var}\left[\sqrt{r_j'^{-n}Y_{\rho,\zeta,1}^\lambda}\right] &= \mathrm{var}[Y_{\rho,\zeta,1}^\lambda]\int_0^R \left(\frac{2r_j}{R^2}\right)dr_j \\
&\times \int_0^{2\pi}\left(\sqrt{3R^2 + r_j^2 - 2\sqrt{3}Rr_j\cos\theta}\right)^{-4}\frac{1}{2\pi}d\theta \qquad (23)
\end{aligned}
$$

According to Gradshteyn and Rizhyk table integrals [31], it is given by:

$$\mathrm{var}\left[\sqrt{r_j'^{-n}Y_{\rho,\zeta,1}^\lambda}\right] = \frac{1}{3N}\frac{1}{4R^4} \qquad (24)$$

Following the forward link case, for the signal to noise plus interference ratio Y_s we obtain:

$$
\begin{aligned}
Y_s &= \left[\frac{2K}{3N}\left(1 + \frac{1}{4R^4}\,\frac{\sum_{l=1}^{L}\beta_{I,li}^2 + \sum_{l=1}^{L}\beta_{J,lj}^2}{\sum_{v=1}^{L}\beta_{B,v1}^2}\right)\right]^{-1} \\
&= \left[\frac{2K}{3N}\left(1 + \frac{1}{4R^4}\,\frac{\chi_I + \chi_J}{\chi_B}\right)\right]^{-1} \qquad (25)
\end{aligned}
$$

letting $\chi_B = \Sigma_{v=1}^L \beta_{B,v1}^2$, $\chi_I = \Sigma_{l=1}^L \beta_{I,li}^2$, and $\chi_J = \Sigma_{l=1}^L \beta_{J,lj}^2$.

The unconditional symbol error probability is given by:

$$P_M = (M-1)\int_0^\infty \frac{1}{2^{2L-1}} \exp\left(\frac{1}{2}\left[\frac{2K}{3N}\left(1+\frac{1}{4R^4}v\right)\right]^{-1}\right) \times \sum_{n=0}^{L-1} c_n \left(\frac{1}{2}\left[\frac{2K}{3N}\left(1+\frac{1}{4R^4}v\right)\right]^{-1}\right) \times \left(\int_0^\infty f_w(uv) f_u(u) du\right) dv \quad (26)$$

where

$$c_n = \frac{1}{n!}\sum_{p=0}^{L-1-n} \binom{2L-1}{p}$$

The symbol error probability can be converted to an equivalent bit error probability P_b by eqn. 17.

4 Imperfect power control

So far, we have assumed that the power control at each mobile within each cell is perfect. In the forward link case, such assumption sounds sensible since the base station transmits the signal in predetermined time moments and the desired level has already been determined by an appropriate handshaking protocol, but this is not the case in the reverse link. The asynchronous mode operation often makes the power control imperfect, and the average received power at the base station is not the same for all users [13, 14]. Hence, we rewrite eqn. 18:

$$\begin{aligned} r(t) =& \eta(t) + \sqrt{2P_S}\varepsilon_1 \Bigg[\sum_{\ell=1}^{L} \beta_{B,\ell 1} s_m^1(t-\tau_{B,\ell 1}) \\ & \times \exp[j\omega_c(t-\tau_{B,\ell 1}) + j(\varphi_{B,\ell 1}+\theta_{B,1})] \\ & + \sum_{k=2}^{K}\sum_{\ell=1}^{L} (\varepsilon_k \beta_{B,\ell k} U_m^k(t-\tau_{B,\ell k}) \\ & \times \exp[j\omega_c(t-\tau_{B,\ell k}) + j(\varphi_{B,\ell k}+\theta_{B,k})])\Bigg] \\ & + \sum_{i=1}^{K}\sum_{\ell=1}^{L} \sqrt{2P_S \partial(r_i')\varepsilon_i'}\, [\beta_{I,\ell i} U_m^i(t-\tau_{I,\ell i}) \\ & \times \exp[j\omega_c(t-\tau_{I,\ell i}) + j(\varphi_{I,\ell i}) + \theta_{I,i})]] \\ & + \sum_{j=1}^{K}\sum_{\ell=1}^{L} \sqrt{2P_S \partial(r_j')\varepsilon_j''}\, [\beta_{l,\ell j} U_m^j(t-\tau_{l,\ell j}) \\ & \times \exp[j\omega_c(t-\tau_{J,\ell j}) + j(\varphi_{J,\ell j}) + \theta_{J,j})]] \end{aligned} \quad (27)$$

where the factors ε_k, ε_i', ε_j'' represent the power control error, and it can be assumed that they are independent random variables uniformly distributed given by [13]

$$f_\varepsilon = \begin{cases} \frac{1}{2V} & \sqrt{2P_S} - V \le \varepsilon \le \sqrt{2P_S} + V \\ 0 & \text{elsewhere} \end{cases} \quad (28)$$

To evaluate the system performance, we have to calculate the mean square value of the last term that is given by

$$E[\varepsilon^2] = (\sqrt{2P_S})^2 + \frac{V^2}{3} \quad (29)$$

As in Section 3, we can conclude that the signal to noise ratio can be given by:

$$\begin{aligned} Y_S &= \left[\frac{2K\left(1+\frac{F_m}{3}\right)}{3N}\left(1+\frac{1}{4R^4}\frac{\sum_{\ell=1}^{L}\beta_{I,\ell i}^2 + \sum_{\ell=1}^{L}\beta_{J,\ell j}^2}{\sum_{v=1}^{L}\beta_{B,v1}^2}\right)\right]^{-1} \\ &= \left[\frac{2K\left(1+\frac{F_m}{3}\right)}{3N}\left(1+\frac{1}{4R^4}\frac{\chi_I+\chi_J}{\chi_B}\right)\right]^{-1} \end{aligned} \quad (30)$$

where $F_m = V^2/(\sqrt{[2P_S]})^2$.

Then, substituting eqn. 30 into eqn. 26, we can determine the error probability for the imperfect power control case:

$$P_M = (M-1)\int_0^\infty \frac{1}{2^{2L-1}} \times \exp\left(\frac{1}{2}\left[\frac{2K\left(1+\frac{F_m}{3}\right)}{3N}\left(1+\frac{1}{4R^4}v\right)\right]^{-1}\right) \times \sum_{n=0}^{L-1} c_n\left(\frac{1}{2}\left[\frac{2K\left(1+\frac{F_m}{3}\right)}{3N}\left(1+\frac{1}{4R^4}v\right)\right]^{-1}\right) \times \left(\int_0^\infty f_w(uv)f_u(u)du\right) dv \quad (31)$$

5 Numerical results and discussion

In the following, we compare and discuss the bit error probability for both the forward and reverse link. For the calculations, we have used random orthogonal codes.

The studied parameters are the number of paths L, the number of symbols per user M, the signal to interference ratio Y_S and the bandwidth efficiency η.

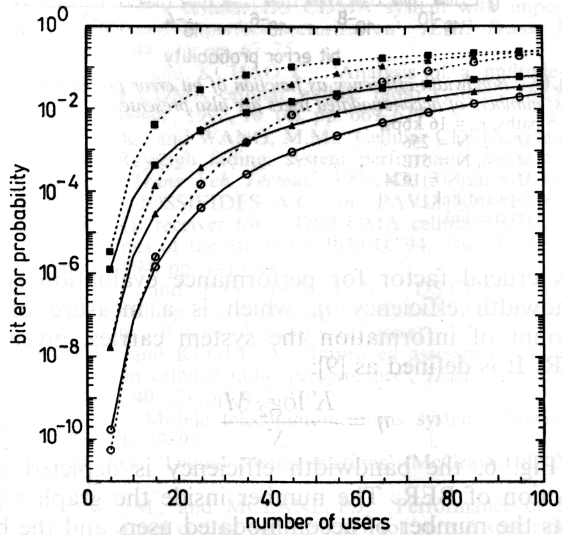

Fig.5 *Bit error probability against number of users over multipath Rayleigh and lognormal shadowing with constant ratio bits per chip*
L = 5 paths, r_b = 16 kbps;
■ M = 2, N = 256
▲ M = 4, N = 512
○ M = 16, N = 1024
—— forward link
······ reverse link

In Fig. 5, the error probability is depicted as a function of the number of accommodated users with $\log_2 M/N$ = 0.0039 bits/chip, namely, an increase of M results in an increase of N when the information rate r_b is kept constant. As expected, the behaviour of the forward link is better than the reverse link, but this depends on the nature of the receivers: coherent or noncoherent. As M increases, and for a low number of users, the performance in both cases is almost the same. The difference in performance becomes significant for a very large number of users (greater than 65). Also, in noncoherent systems, there is a saturation point where the system performance is independent of M, but in both the systems, we can achieve transfer of safely data (BER less than 10^{-6}) for different values of M. Given the number of users (e.g. $K = 14$) this can be achieved for both the links with $M = 16$ and $N = 1024$. At large values of M, the benefits of M-ary signalling are presented. For the voice quality limit $P_b = 10^{-3}$, the results are very different for the two links. In the forward link, and for $M = 4$, the limit can be achieved with $K = 33$ accommodated users while, in the reverse link, the number of accommodated users is only $K = 21$. In the reverse link, if we desire to achieve the same value in BER with 35 users, we have to increase M and N simultaneously ($M = 16$, $N = 1024$).

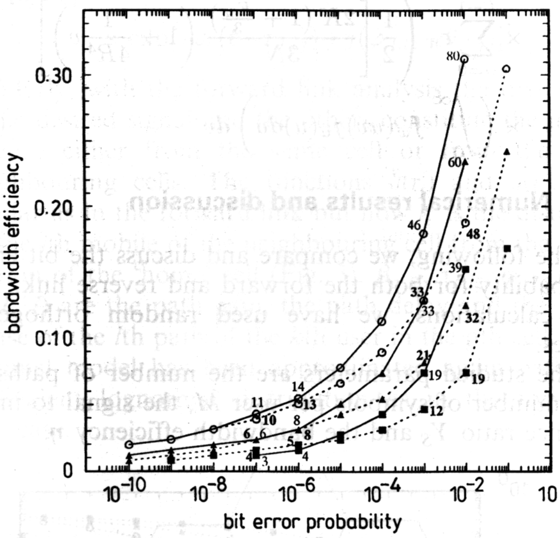

Fig. 6 *Bandwidth efficiency as function of bit error probability for both links; numbers of accommodated users are also presented*
$L = 5$ paths, $r_b = 16$ kbps;
—■— $M = 2$, $N = 256$
—▲— $M = 4$, $N = 512$
—○— $M = 16$, $N = 1024$
——— forward link
········· reverse link

A crucial factor for performance evaluation is the bandwidth efficiency η, which is a measure of the amount of information the system carries, given the BER. It is defined as [9]:

$$\eta = \frac{K \log_2 M}{N} \tag{32}$$

In Fig. 6, the bandwidth efficiency is depicted as a function of BER. The number inside the graph represents the number of accommodated users and the bold type numbers give the accommodated users in the reverse link. Maximum bandwidth efficiency equal to 0.3125 is observed in the forward link for the maximum value of M and for the maximum length of spreading sequences N. Hence, the impact of the increased complexity (large M and N) is more beneficial in the forward link.

The number of accommodated users is a function of the number of resolvable paths L (Fig. 7). Assuming only one path, the performance in both the links is similar and very poor. Taking advantage of the inherent property of spread spectrum (implicit diversity), the system's performance enhances but depends on the number of users. Therefore, the safe limit for data transfer can be obtained for up to 15 users in the forward link and ten users in the reverse link considering more than five taps in the RAKE receiver, but there is an important difference between the two links. In the reverse link, the increase in the number of resolvable paths is positive until the system approaches a critical point (at about 32 users). Above this point, the impact becomes negative and the multiple access dominates the increased path resolvability. On the contrary, in the forward link, increasing L gives an improvement of the system's performance, but the improvement is not significant for $L > 5$ in comparison with the increased system complexity. The same result also arises in the reverse link but only for number of users less than 32.

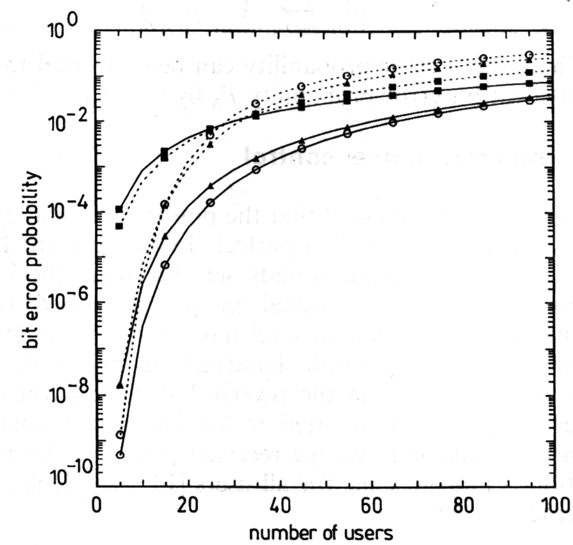

Fig. 7 *BER against simultaneous users with wide range of number of resolvable paths*
$M = 4$ symbols/user, $N = 512$
—■— $L = 1$ path
—▲— $L = 5$ paths
—○— $L = 8$ paths
——— forward link
········· reverse link

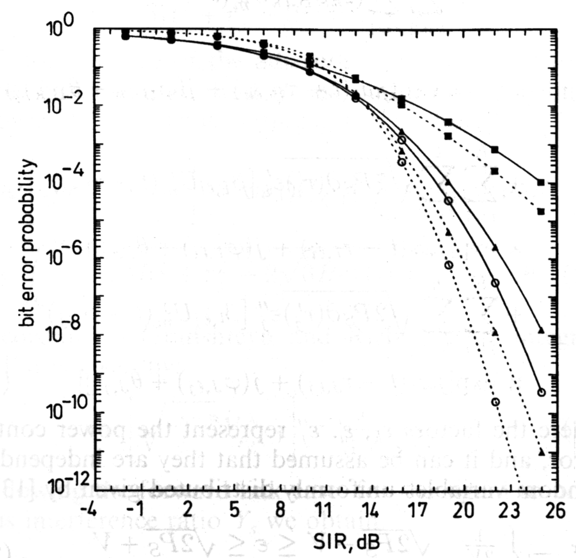

Fig. 8 *BER against SIR with different number of resolvable paths*
$M = 4$ symbols/user, $N = 512$
—■— $L = 1$ path
—▲— $L = 5$ paths
—○— $L = 8$ paths
——— forward link
········· reverse link

In Fig. 8 the error probability as a function of γ_S is presented with the number of resolvable paths as the parameter. Increasing γ_S enhances the system. In the medium γ_S area, a difference of 3dB gives about two orders of improvement in BER. The level of 8dB gives another aspect of the result stated in the previous paragraph.

Finally, Fig. 9 depicts the performance of the system against RMS delay spread for a variety of power control errors. The three curves correspond to $F_m = 0$ (perfect power control), $F_m = 0.707$ (variation ±50% about its nominal value) and $F_m = 1.0$ (±100% variation). We can notice that, as the power control error increases, the bit error probability also increases. In particular, when the power control error overcomes ±50%, the degradation in system performance is large enough and closed loop power control algorithms have to be applied [32]. Another point is that an RMS delay spread increase results in a decrease of BER, since the signal energy disperses through a large number of paths and it is difficult for it to be picked up, without noise assemblage (multiple access interference plus noise) at the same time. Therefore, there is no need to increase the number of resolvable paths. For any non-coherent system, an optimum point of L can be found [22] ($L = 3$ in our case).

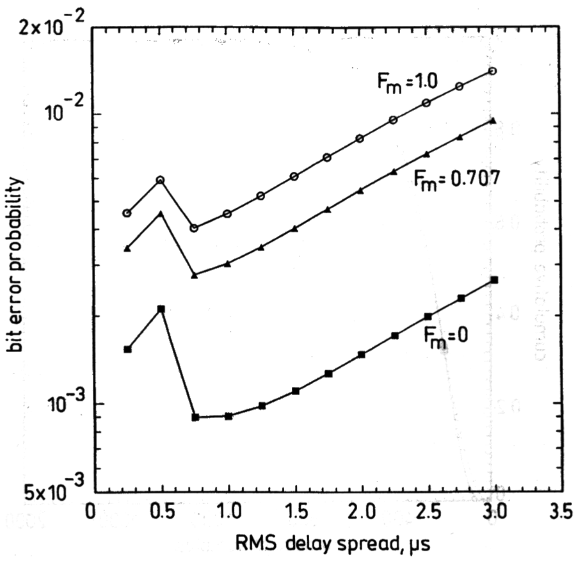

Fig. 9 *BER against RMS delay spread in reverse link for different power control errors*
$K = 20$ users, $M = 4$, $N = 512$, $r_b = 16$ kbps

6 Conclusions

A cluster analysis for both the links (uplink and downlink) of an M-ary DS/CDMA orthogonal signalling system has been presented. The channel model is considered to be frequency selective with multipath Rayleigh fading and lognormal shadowing. The proposed system has been evaluated in terms of BER. As far as we know, this is the first time that such an analysis in a wideband environment has taken place. A RAKE receiver, namely a coherent type with MRC in the forward link and a noncoherent type with square law combiner, was applied in both the links, taking into consideration the implicit diversity. Also, a very satisfactory approximation of the channel model has been achieved, approaching the Rayleigh-lognormal distribution with an equivalent lognormal. The imperfect power control case has been studied giving us an in-depth insight of the system. The mathematical analysis is quite general and can be applied in any number of resolvable paths. The positive results in both the links, encourage us to insist on a M-ary DS/CDMA orthogonal signalling as the future in PCN.

7 References

1 SIMON, M.K., OMURA, J.K., SCHOLTZ, R.A., and LEVITT, B.K.: 'Spread spectrum communications' (Computer Science Press, Rockville, MD, 1985), vol. 3

2 VITERBI, A.J.: 'Implications of mobile cellular CDMA', *IEEE Commun. Mag.*, 1992, **30**, (12), pp. 38–41

3 SCHILLING, D.L., MILSTEIN, L.B., PICKHOLTZ, R.L., KULLBACK, M., and MILLER, F.: 'Spread spectrum for commercial communications', *IEEE Commun. Mag.*, 1991, **29**, (4), pp. 66–79

4 PICKHOLTZ, R.L., MILSTEIN, L.B., and SCHILLING, D.L.: 'Spread spectrum for mobile communications', *IEEE Veh. Technol.*, 1991, **40**, (2), pp. 303–312

5 AGHVAMI, A.H.: 'Future CDMA cellular mobile systems supporting multi-service operation'. Proceedings of the 5th IEEE PIMRC'94, The Hague, The Netherlands, 1994, pp. 1276–1279

6 SCHILLING, D.L.: 'Wireless communications going into the 21st century', *IEEE Trans. Veh. Technol.*, 1994, **43**, (3), pp. 645–652

7 ENGE, P.K., and SARWATE, D.V.: 'Spread spectrum multiple-access performance of orthogonal codes: linear receiver', *IEEE Trans.*, 1987, **COM-35**, (12), pp. 1309–1319

8 CHASE, M., and PAHLAVAN, K.: 'Performance of DS-CDMA over measured indoor radio channels using random orthogonal codes', *IEEE Trans. Veh. Technol.*, 1993, **42**, (4), pp. 617–624

9 PAHLAVAN, K., and CHASE, M.: 'Spread-spectrum multiple access performance of orthogonal codes for indoor radio communications', *IEEE Trans. Commun.*, 1990, **38**, (5), pp. 574–577

10 JALLOUL, L.M.A., and HOLTZMAN, J.M.: 'Performance analysis of DS/CDMA with noncoherent M-ary orthogonal modulation in multipath fading channels', *IEEE J. Sel. Areas Commun.*, 1994, **12**, (5), pp. 862–870

11 LEE, W.C.Y.: 'Overview of cellular CDMA', *IEEE Trans. Veh. Technol.*, 1991, **40**, (2), pp. 291–302

12 GILHOUSEN, K.S., JACOBS, I.M., PADOVANI, R., WEAVER, L.A., and WHEATLEY III, C.E.: 'On the capacity of cellular CDMA system', *IEEE Trans. Veh. Technol.*, 1991, **40**, (2), pp. 303–312

13 MILSTEIN, L.B., RAPPAPORT, T.S., and BARGHOUTI, R.: 'Performance evaluation for cellular CDMA', *IEEE J. Sel. Areas Commun.*, 1992, **10**, (4), pp. 680–689

14 MISSER, H.S., and PRASAD, R.: 'Bit error probability evaluation of a microcellular spread-spectrum multiple access system in a shadowed Rician fading channel'. Proceedings of the 42nd IEEE *Vehicle technology* conference, Denver, CO, 1992, pp. 43–46

15 JANSEN, M.G., and PRASAD, R.: 'Capacity, throughput, and delay analysis of a cellular DS CDMA system with imperfect power control and imperfect sectorization', *IEEE Trans. Veh. Technol.*, 1995, **44**, (1), pp. 67–75

16 STUBER, G.L., and KCHAO, C.: 'Analysis of a multiple-cell direct-sequence CDMA cellular mobile radio system', *IEEE J. Sel. Areas Commun.*, 1992, **10**, (4), pp. 669–679

17 TONGUZ, O.K., and WANG, M.M.: 'Cellular CDMA networks impaired by Rayleigh fading: system performance with power control', *IEEE Trans. Veh. Technol.*, 1994, **43**, (3), pp. 515–527

18 DALLAS, P.I., IOSSIFIDES, A.C., and PAVLIDOU, F.-N.: 'A modified RAKE receiver for a DS/CDMA cellular mobile system'. Proceedings of the 5th IEEE PIMRC'94, The Hague, The Netherlands, 1994, pp. 1419–1423

19 DALLAS, P.I., and PAVLIDOU, F.-N.: 'DS/CDMA M-ary orthogonal signalling in a shadowed Rayleigh channel for mobile communications', *Wireless Networks*, (in press)

20 PRASAD, R., and KEGEL, A.: 'Improved assessment of interference limits in cellular radio performance', *IEEE Trans. Veh. Technol.*, 1991, **40**, (2), pp. 412–419

21 LEE, W.C.Y.: 'Mobile telecommunications system' (McGraw-Hill, New York, 1989)

22 PROAKIS, J.G.: 'Digital communications' (McGraw-Hill, New York, 1989)

23 KAVEHRAD, M., and MCLANE, P.J.: 'Performance of low-complexity channel coding and diversity for spread spectrum in indoor, wireless communication', *AT&T Techn. J.*, 1985, **64**, (8), pp. 1927–1964

24 PURSLEY, M.B.: 'Spread spectrum multiple access communications' *in* LONGO, G. (Ed.): 'Multi-user communications systems' (Springer-Verlag, New York, 1981), pp. 139–199

25 GERANIOTIS, E.A., and PURSLEY, M.B.: 'Performance of noncoherent direct-sequence CDMA systems', *IEEE Trans.*, 1986, **COM-34**, (3), pp. 219–226

26 WEI, L.: 'Estimated bit-error probability of DS-SSMA/MPSK with coherent detector on satellite mobile channel', *IEEE J. Sel. Areas Commun.*, 1995, **13**, (2), pp. 250–262

27 PAPOULIS, A.: 'Probability, random variables and stochastic processes' (McGraw-Hill, New York, 1991)

28 ARNBAK, J.C., and VAN BLITTERSWIJK, W.: 'Capacity of slotted Aloha in Rayleigh channels', *IEEE J. Sel. Areas Commun.*, 1987, **5**, (2), pp. 261–269

29 ABU-DAYYA, A.A., and BEAULIEU, N.C.: 'Outage probabilities in the presence of correlated lognormal interferers', *IEEE Trans. Veh. Technol.*, 1994, **43**, (1), pp. 164–173

30 SCHWARTZ, S.C., and YEH, Y.S.: 'On the distribution function and moments of power sums with lognormal components', *Bell Syst. Tech. J.*, 1982, **61**, (7), pp. 1441–1462
31 GRADSHTEYN, I., and RYZHIC, I.M.: 'Tables of integrals, series and products' (Academic Press, New York, 1980)
32 VITERBI, A.J., VITERBI, A.M., and ZEHAVI, E.: 'Performance of power controlled wideband terrestrial digital communication', *IEEE Trans. Commun.*, 1993, **41**, (4), pp. 559–569
33 JIRATTITICHAREON, A., and FARELL, T.O.: 'Analysis of DS/SSMA for indoor radio communication in a log-normal fading channel', *Electron. Lett.*, 1993, **29**, (13), pp. 1204–1206

8 Appendix

In the following, we wish to prove that the joint probability density function (PDF) of Rayleigh-lognormal can be approximated by an equivalent lognormal distribution by the appropriate transformation in mean and standard deviation according to a previous publication [20]. First, we calculate the first and the second moment of both the distributions and then we apply the cumulant matching approach [29].

The PDF of multipath Rayleigh and lognormal shadowing can be given by [19]:

$$f_{RL}(y) = \int_0^\infty \frac{1}{X^L(L-1)!} y^{L-1} \exp\left(-\frac{y}{x}\right) \times \frac{1}{\sigma x\sqrt{2\pi}} \exp\left(-\frac{(\ln x - \xi)^2}{2\sigma^2}\right) dx \quad (33)$$

The mean value is defined as:

$$E[y] = \int_0^\infty y \left(\int_0^\infty \frac{1}{X^L(L-1)!} y^{L-1} \exp\left(-\frac{y}{x}\right) \times \frac{1}{\sigma x\sqrt{2\pi}} \exp\left(-\frac{(\ln x - \xi)^2}{2\sigma^2}\right) dx\right) dy \quad (34)$$

According to [19, 22], the above can be simplified to:

$$E[y] = \int_0^\infty Lx \frac{1}{\sigma x\sqrt{2\pi}} \exp\left(-\frac{(\ln x - \xi)^2}{2\sigma^2}\right) dx \quad (35)$$

This equals L times the mean value of lognormal distribution so:

$$E[y] = L \exp\left(\xi + \frac{\sigma^2}{2}\right) \quad (36)$$

Similarly, the mean square value can be written by:

$$E[y^2] = L(L+1)\exp(2\xi + 2\sigma^2) \quad (37)$$

The mean value and the mean square value of a lognormal distribution can be given, respectively, by [33]:

$$E[x] = \exp\left(\xi_L + \frac{\sigma_L^2}{2}\right) \quad (38)$$

and

$$E[x^2] = \exp(2\xi_L + 2\sigma_L^2) \quad (39)$$

Matching the first moment, one obtains:

$$\exp\left(\xi_L + \frac{\sigma_L^2}{2}\right) = L\exp\left(\xi + \frac{\sigma^2}{2}\right) \quad (40)$$

The second moment matching gives:

$$\exp(2\xi_L + 2\sigma_L^2) = L(L+1)\exp(2\xi + 2\sigma^2) \quad (41)$$

Solving the linear system results:

$$\xi_L = \xi + \ln\left(\sqrt{\frac{L^3}{L+1}}\right) \quad (42)$$

and

$$\sigma_L^2 = \sigma^2 + \ln\left(\frac{L+1}{L}\right) \quad (43)$$

For $L = 1$, the previous equations comply with [20].

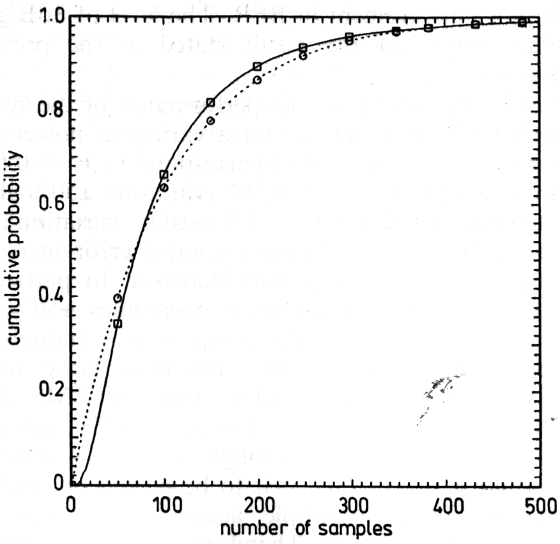

Fig. 10 *Comparison between Rayleigh-lognormal and equivalent lognormal for L = 1*
—□— Rayleigh-lognormal
- -○- - lognormal approximation

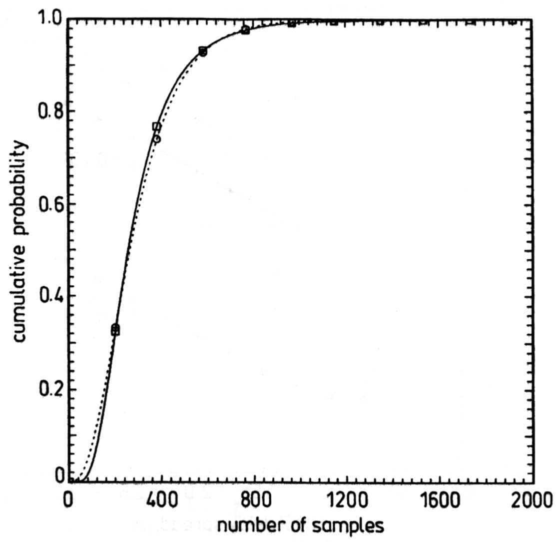

Fig. 11 *Comparison between Rayleigh-lognormal and equivalent lognormal for L = 3*
—□— Rayleigh-lognormal
- -○- - lognormal approximation

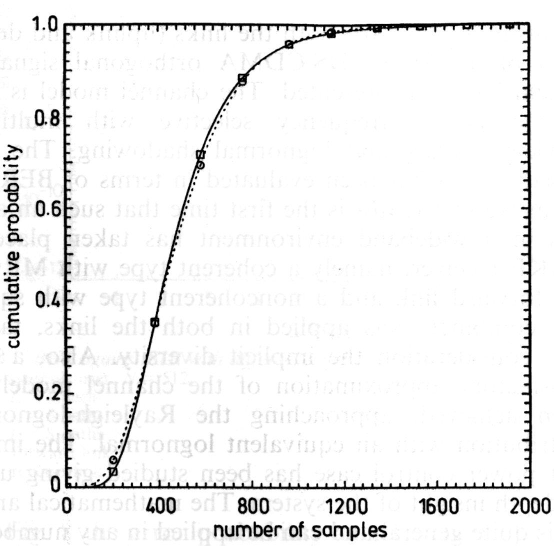

Fig. 12 *Comparison between Rayleigh-lognormal and equivalent lognormal for L = 5*
—□— Rayleigh-lognormal
- -○- - lognormal approximation

Verifying the above approximation, we present some simulation results comparing the two PDFs (Figs. 10–12). The simulation was developed in C++ and run on HP 9000/735. Also, the Kolmogorov–Smyrnov test was applied and it proved that, as the number of paths increases the approximation becomes better. For $L = 5$, the confidence interval is less than 0.01 while, for $L = 3$, the approximation is slightly higher than the appropriate Kolmogorov–Smyrnov limit for 0.05 as a confidence interval. Finally, we present the $L = 1$ case, although the results are not very satisfactory. The number of paths is the crucial factor that affects the quality of the approximation because the number of the paths is involved both in the mean value and in the standard deviation.